DOI: 10.6060/ivkkt.20246712.7081

УДК: 537.525

ПАРАМЕТРЫ ПЛАЗМЫ И КИНЕТИКА РЕАКТИВНО-ИОННОГО ТРАВЛЕНИЯ ZnO В БРОМИСТОМ ВОДОРОДЕ: ВЛИЯНИЕ ИНЕРТНОГО ГАЗА-НОСИТЕЛЯ

А.М. Ефремов, С.А. Смирнов, В.Б. Бетелин, К.-Н. Kwon

Александр Михайлович Ефремов (ORCID 0000-0002-9125-0763)*

НИИМЭ, ул. Академика Валиева, 6/1, Зеленоград, Москва, Российская Федерация, 124460
E-mail: amefremov@mail.ru*

Сергей Александрович Смирнов (ORCID 0000-0002-0375-0494)

Ивановский государственный химико-технологический университет, Шереметевский пр., 7, Иваново, Российская Федерация, 153000
E-mail: sas@isuct.ru

Владимир Борисович Бетелин (ORCID 0000-0001-6646-2660)

ФГУ ФНЦ НИИСИ РАН, Нахимовский пр., 36, к.1, Москва, Российская Федерация, 117218
E-mail: betelin@niisi.msk.ru

Kwang-Ho Kwon (ORCID 0000-0003-2580-8842)

Korea University, 208 Seochang-Dong, Chochiwon, Korea, 339-800
E-mail: kwonkh@korea.ac.kr

В работе обсуждается влияние инертных газов-носителей, Ar и He, на характеристики газовой фазы и скорость травления ZnO в типичных условиях реактивно-ионного травления в плазме бромистого водорода. Диагностика плазмы с помощью зондов Ленгмюра и 0-мерное моделирование плазмы позволили выяснить, как содержание данного газа-носителя влияет на параметры электронной и ионной компонент плазмы, кинетику активных частиц и их концентрации. Было обнаружено, что переход к смесям с высоким содержанием Ar или He а) вызывает рост температуры электронов (из-за меньших потерь энергии электронов при столкновениях с атомными частицами); б) снижает электроотрицательность плазмы и в) приводит к противоположным изменениям как концентрации, так и плотности потока ионов. Последнее явление обусловлено противоположными изменениями суммарных скоростей ионизации из-за существенной разницы в коэффициентах скоростей ионизации Ar и He. Важными особенностями плазмы HBr + Ar при 0-80% Ar также являются более медленное, чем линейное, падение концентрации атомов Br (из-за интенсификации диссоциации молекул HBr и Br_2 электронным ударом), а также увеличение концентрации атомов H (из-за снижения скорости их гибели в газовой фазе). Эксперименты по травлению показали, что скорость травления ZnO формируется, в основном, ионно-стимулированной химической реакцией, при этом скорость реакции снижается быстрее по сравнению с плотностью потока атомов брома. Соответствующее снижение эффективной вероятности может быть связано как с изменением интенсивности ионной бомбардировки, так и с эффектом водородной пассивации.

Ключевые слова: HBr, Ar, He, плазма, параметры, активные частицы, ионизация, диссоциация, травление, вероятность реакции

Для цитирования:
Ефремов А.М., Смирнов С.А., Бетелин В.Б., Kwon К.-Н. Параметры плазмы и кинетика реактивно-ионного травления ZnO в бромистом водороде: влияние инертного газа-носителя. *Изв. вузов. Химия и хим. технология*. 2024. Т. 67. Вып. 12. С. 86–95. DOI: 10.6060/ivkkt.20246712.7081.

For citation:
Efremov A.M., Smirnov S.A., Betelin V.B., Kwon K.-H. Plasma parameters and reactive-ion etching kinetics of ZnO in hydrogen bromide: the influence of inert carrier gas. *ChemChemTech [Izv. Vyssh. Uchebn. Zaved. Khim. Khim. Tekhnol.]*. 2024. V. 67. N 12. P. 86–95. DOI: 10.6060/ivkkt.20246712.7081.

PLASMA PARAMETERS AND REACTIVE-ION ETCHING KINETICS OF ZnO IN HYDROGEN BROMIDE: THE INFLUENCE OF INERT CARRIER GAS

A.M. Efremov, S.A. Smirnov, V.B. Betelin, K.-H. Kwon

Alexander M. Efremov (ORCID 0000-0002-9125-0763)*

Molecular Electronics Research Institute (MERI), Academic Valiev st., 6/1, Zelenograd, Moscow, 124460, Russia
E-mail: amefremov@mail.ru*

Sergey A. Smirnov (ORCID 0000-0002-0375-0494)

Ivanovo State University of Chemistry and Technology, Sheremetevskiy ave., 7, Ivanovo, 153000, Russia
E-mail: sas@isuct.ru

Vladimir B. Betelin (ORCID 0000-0001-6646-2660)

SRISA RAS, Nakhimovsky ave., 36, bld. 1, Moscow, 117218, Russia
E-mail: betelin@niisi.msk.ru

Kwang-Ho Kwon (ORCID 0000-0003-2580-8842)

Korea University, 208 Seochang-Dong, Chochiwon, Korea, 339-800
E-mail: kwonkh@korea.ac.kr

This work discusses the influence of inert carrier gases, Ar and He, on both gas-phase plasma characteristics and ZnO etching rate under typical reactive-ion etching conditions in the hydrogen bromide environment. Plasma diagnostics by Langmuir probes and 0-dimensional plasma modeling allowed one to compare how the content of given carrier gas does influence electrons-and ions-related plasma parameters, kinetics and densities of plasma active species. It was found that the transition toward Ar- or He-rich plasmas a) causes the growth of electron temperature (due to lower electron energy losses in collisions with atomic species); b) reduces plasma electronegativity; and c) results in opposite changes in both ion density and ion flux. The last phenomenon is due to opposite changes in total ionization rates determined by sufficient difference in ionization rate coefficients for Ar and He atoms. Important features of HBr + Ar plasma at 0–80% Ar are also the slower-than-linear fall of Br atom density (due to the intensification of electron impact dissociation for both HBr and Br_2 molecules) as well as an increase in H atom density (due to decreasing their loss rate in gas-phase reactions). Etching experiments indicated that the ZnO etching rate is mostly contributed by the ion-assisted chemical reaction while the reaction rate decreases faster compare with the Br atom flux. The corresponding decrease in the effective reaction probability may be related to changes in both ion bombardment intensity and hydrogen passivation effect.

Keywords: HBr, Ar, He, plasma, parameters, active species, ionization, dissociation, etching, reaction probability

INTRODUCTION

Halogen-containing gases play the remarkable role in modern in the micro- and nano-electronic technology being used for patterning (dimensional etching) of both silicon wafers and various functional layers [1–3]. The commonly used tool here is the reactive-ion etching (RIE) technique in a combination with the inductively-coupled plasma (ICP) etching system [4, 5]. Corresponding features are a) the simultaneous action of physical (the sputtering of surface atoms by energetic ions) and chemical (the gasification of surface atoms in a form of volatile reaction products) etching pathways; and b) the possibility of independent control for ion flux and ion energy. All these provide the flexible adjustment of output process characteristics in respect to etching rate, etching selectivity and anisotropy [5, 6].

Among the variety of gases involved in RIE processes, the noticeable place is occupied by hydrogen bromide. First, HBr is the preferable active gas for etching of III-V semiconductor materials, such as GaAs, InGaAs and InP. As corresponding bromides (in spite of fluorides or chlorides) are characterized by nearly equal volatilities at typical process tempera-

tures, one can obtain the nearly stoichiometric composition of the etched surface [7, 8]. And secondly, the HBr itself as well as HBr + O_2 gas mixtures have successfully been applied to the highly-anisotropic etching of silicon to produce high-aspect-ratio structures [9–11]. The mechanisms providing such effect are the negligible spontaneous reaction between Br and Si atoms as well as the passivation of sidewalls by low volatile $SiBr_xO_y$ compounds [12, 13]. Another important feature is that HBr is frequently used not as an individual compound, but appears in a mixture with the inert carrier gas, mostly with Ar. The roles of carrier gas are to stabilize plasma, to increase the spatial uniformity of plasma parameters, to intensify ion-assisted heterogeneous processes and, finally, to decrease the content of chemically active species in the outcoming gas flow. The latter helps to prevent the damage of pumping equipment and weakens environmental protection requirements. Accordingly, there were several works focused on relationships between processing conditions and plasma chemistry determining steady-state densities of plasma active species in HBr + Ar mixtures [14–17]. When summarizing existing data, one can conclude that the transition toward Ar-rich plasmas a) enriches the electron energy distribution function by high-energy electrons; b) causes an increase in total ionization rate and plasma density; c) changes the formation/decay balance for Br and H atoms and d) accelerates both chemical and the physical etching pathways due to the growth of ion flux. Surprisingly, the almost no attention was attracted to HBr + He gas system. At the same time, He exhibits the extremely high heat conductivity coefficient [18] and thus, provides the fast heat transfer from gas to chamber walls. It can be suggested that such situation flattens gas temperature and density profiles, equalizes fluxes of plasma active species along the radial direction and, finally, increases the spatial uniformity of etching process. Therefore, the investigation of plasma features HBr + He mixture as well as the comparative study of HBr + Ar and HBr + He plasmas at identical processing conditions are actual tasks to provide the correct choice of carrier gas for the given etching process.

Previously, Gul et al. [19] has made an attempt to compare of HBr + Ar and HBr + He mixtures under the condition of capacitive coupled plasma. Unfortunately, their model-based study has the somewhat limited value, as was performed at high pressures (150 mtor, that is really far from conventional RIE conditions), was not matched with any experimental data as well as was based on strange reaction set with no surface loss processes for atomic and ionic species. In particular, exactly the last feature resulted in abnormally high HBr dissociation degrees at low (~ 10^9 cm^{-3}) electron densities. The aim of this work was to compare HBr + Ar and HBr + He plasmas under typical RIE conditions in respect to gas-phase parameters and ZnO etching process. For this purpose, we suggested to use well-adjusted kinetic schemes and modeling algorithm which were tested in our previous works and have demonstrated the satisfactory agreement with experiments [14, 15]. The interest to ZnO is because it represents a promising semiconductor material for blue/UV light emitting diodes, spintronics devices, surface acoustic wave devices and gas sensors [20, 21]. Among many gas chemistries studied for dry patterning of ZnO thin films, the HBr-based ones received minor attention. As such, we were mainly focused on the questions how both type and content of carries gas do influence plasma parameters and densities of active species responsible for ZnO etching kinetics.

EXPERIMENTAL AND MODELING DETAILS

Experimental setup and conditions

Experiments were performed in the planar (with the upper-side flat cooper coil) inductively-coupled plasma (ICP) reactor [14–16]. Plasma was excited in HBr +Ar and HBr + He gas mixtures using the 13.56 MHz power supply at constant total gas flow rate (q = 40 sccm), gas pressure (p = 6 mtor) and input power (W = 700 W). The single variable parameter was the HBr/inert gas mixing ratio which was set by adjusting partial gas flow rates for mixture components. Accordingly, an increase in Ar (q_{Ar}) or He (q_{He}) flow rates from 0–30 sccm corresponded to the change in corresponding gas fractions, y_{Ar} or y_{He}, in the range of 0–75%.

Plasma diagnostics was performed by double rf-compensated Langmuir probe (LP) DLP2000 (Plasmart Inc.). The probe head was installed through the chamber wall-side view port, placed at 4 cm above the chuck electrode and centered in the radial position. The treatment of measured voltage-current curves was based on well-known statements of Langmuir probe theory for low pressure plasmas [6, 22]. As a result, we obtained electron temperature (T_e) and ion current density (J_+).

For the study of ZnO etching kinetics, we used fragments of Si (001) wafer with preliminary deposited 180-nm thick ZnO film. The film was produced using rf-magnetron sputtering of the 99.99% ZnO target in the 20 sccm Ar+10 sccm O_2 gas mixture. Etched samples with an average size of ~ 2×2 cm were placed in the center of the chuck electrode, and the latter was powered by an independent rf (13.56 MHz) generator to produce the negative dc bias voltage, $-U_{dc}$. As the

bias power source operated in the constant bias power mode (W_{dc} = 200 W), the parameter $-U_{dc}$ (and thus, the ion bombardment energy) was sensitive to gas-phase plasma characteristics through the change in ion flux. The chuck electrode was equipped by the water-flow cooling system that stabilized its temperature at ~ 20 °C during the "plasma on" time. The ZnO etching rates were determined as $R = \Delta h/\tau$, where τ is the processing time, and Δh is the thickness of removed layer (the so-called etched depth). The latter was measured using a surface profiler (Alpha-step 500, Tencor). For this purpose, we developed the line striping of the photoresist AZ1512 with the line/space ratio of 2 μm/2 μm. In preliminary experiments, it was found that there are no differences in plasma diagnostics data a) with and without sample loading; b) with increasing number of simultaneously loaded samples; and c) with and without bias power applied to the chuck electrode. Based on these data, one can neglect the disturbance of plasma parameters by the etching products as well as assign plasma as the steady-state source of active species. Another important conclusion is that our etching system represents a kind of "classical" ICP etcher that allows one the independent adjustment of ion flux and ion energy.

In both plasma diagnostics and etching experiments, each individual measurement was repeated by 5 times, and the data were averaged before their plotting. Since the sample loading process assumed the short expose of inner chamber environment with an atmospheric air, each new etching experiment was mandatory started from the chamber conditioning in 50% Ar + 50% O_2 plasma. Accordingly, the same procedure was also used in LP measurements aimed at providing the same state of chamber walls. Typical deviations in respect to average values were always below 10% in the case of etched depth as well as were around 5% in LP measurements.

0-Dimensional plasma model

To investigate how both type and content of inert carrier gas do influence kinetics and densities of plasma active species, we applied a simplified 0-dimensional (global) model. The model accounted for 5 kinds of neutral ground-state species (HBr, H, Br, H_2, Br_2 and Ar or He) as well as for 6 types of ions (HBr^+, H^+, Br^+, Br^-, H_2^+, Br_2^+ and Ar^+ or He^+). Both kinetic scheme (the set of reactions with rate coefficients) and approaches for modeling algorithm were taken from our previous works dealt with HBr-based plasmas [14, 15]. As those have reported the satisfactory agreement between measured and model-predicted plasma parameters, corresponding questions will not be discussed in a framework of given study. In particular, it was suggested that:

- the electron energy distribution function (EEDF) has the nearly Maxwellian shape. Accordingly, rate coefficients for electron-impact reactions may be found using Arrhenius-like equations $k = AT_e^B\exp(-C/T_e)$ resulting from the integration of Maxwellian EEDF with known process cross-sections [15].
- the total density of positive ions appears as $n_+ \approx \Gamma_+/0.61(eT_e/m_i)^{1/2}$ [6, 15], where $\Gamma_+ \approx J_+/e$ is the ion flux, $(eT_e/m_i)^{1/2}$ is the velocity of ions on the plasma sheath edge (the so-called Bohm velocity), and m_i is the effective (ion-type-averaged) ion mass. The latter may be evaluated through individual masses and fractions of positive ions, as was suggested in Refs. [15].
- the electron density is matched with n_+ through the balance equation for negative ions and quasi-neutrality condition, $n_+ = n_e + [Br^-]$. This allows one to obtain $n_e \approx k_3n_+^2/(k_3n_+ + k_1[HBr] + k_2[Br_2])$, where k_1, k_2 and k_3 are rate coefficients for R1: $HBr + e \rightarrow H + Br^-$; R2: $Br_2 + e \rightarrow Br + Br^-$ and R3: $Br^- + X^+ \rightarrow$ neutral products, where X^+ is any positive ion.
- the average temperature of neutral species, T_{gas}, determining their total density in plasma $N = p/k_BT_{gas}$ appears to be independent on both type and content of carrier gas. The modeling procedure was performed with T_{gas} ~ 600 K, as follows from experimental data for pure HBr [23] and Ar [24] plasmas at comparable with our case level of input power density.

RESULTS AND DISCUSSION

From plasma diagnostics by Langmuir probes and plasma modeling, it was found that that increases in Ar and He mixing ratios result in non-identical changes in electrons- and ions-related plasma parameters (Fig. 1). With accounting for model-predicted data on steady-state densities of neutral species (Fig. 2) and previous research experience of binary mixtures combining molecular and noble gases [14, 15, 25–27], corresponding results may be explained as follows:

1) A growth of electron temperature toward Ar- and He-rich plasmas (3.0–3.1 eV for 0–75% Ar and 3.0–3.8 eV for 0–75% He, see Fig. 1(a)) surely reflects a decrease in electron energy losses in both elastic and inelastic collisions. The first effect is because momentum transfer cross-sections for Ar (~ $6.8\cdot10^{-16}$ cm^2 at 3 eV) and He (~ $1.5\cdot10^{-16}$ cm^2 at 3 eV) are sufficiently lower compared with that for HBr (~ $2.2\cdot10^{-15}$ cm^2 at 3 eV) [28, 29]. That is why the decreasing fraction of HBr in a feed gas directly reduces electron energy losses in the low-energy part of EEDF. The second phenomenon originates from the sufficient difference between first excitation potentials for

Ar (~ 11.6 eV) and He (~ 19.8 eV) atoms from one side and molecular plasma components, such as HBr, Br_2 and H_2 (below 0.5 eV for vibrational excitation and below 5 eV for electronic excitation [28, 29]), from the other side. As such, an increase in both y_{Ar} and y_{He} shrinks the electron energy loss range in inelastic collisions, lowers the overall electron energy loss and enriches EEDF by high-energy electrons. The higher effect for HBr + He plasma is due to higher threshold energies and lower absolute cross-section for excitation and ionization of He atoms compared with those for Ar [28, 29].

2) Opposite changes in ion current densities (1.63–4.03 mA/cm^2 for 0–75% Ar and 1.63–1.44 mA/cm^2 for 0–75% He, see Fig. 1(b)) reflect similar behaviors of total positive ion densities (Fig. 1(c)). Thought both gas systems exhibit nearly equal total ionization frequencies (the sum of ionization rate coefficients multiplied by partial densities of corresponding neutral species, ν_{iz}) vs. the fraction of carried gas ($5.6\cdot10^4$–$4.9\cdot10^4$ s^{-1} for 0–75% Ar and $5.6\cdot10^4$–$4.3\cdot10^4$ s^{-1} for 0–75% He), the HBr + Ar plasma is featured by both deeper fall of plasma electronegativity (Fig. 1(d)) (due to higher dissociation degrees for HBr and Br_2 species) and weaker growth of electron diffusion coefficient (due to the weaker change in T_e). Accordingly, the addition of Ar causes the noticeable increase in both electron density (by ~ 4 times at 0–75% Ar, see Fig. 2(c)) and total ionization rate $\nu_{iz}n_e$ providing the formation of positive ions. In spite of this, the addition of He sufficiently accelerates the diffusion of electrons toward chamber walls as well as keeps the higher contribution of dissociative attachment processes R1 and R2 to the total electron loss rate. All these lead to the only weak increase in n_e as well as cause the nearly constant total ionization rate. At the same time, the density of positive ions demonstrates a weak decrease vs. y_{He} due to an increase in ion Bohm velocity.

3) Similar decreasing tendencies for both absolute and relative (Fig. 1(d)) densities of negative ions are generally due to decreasing content of electronegative component in a feed gas. A bit higher electronegativity of HBr + He plasma at $y_{He} = y_{Ar}$ is due to higher formation rate for Br^- ions in R1 and R2 provided by higher densities of corresponding source species, as can be seen from Fig. 2(a).

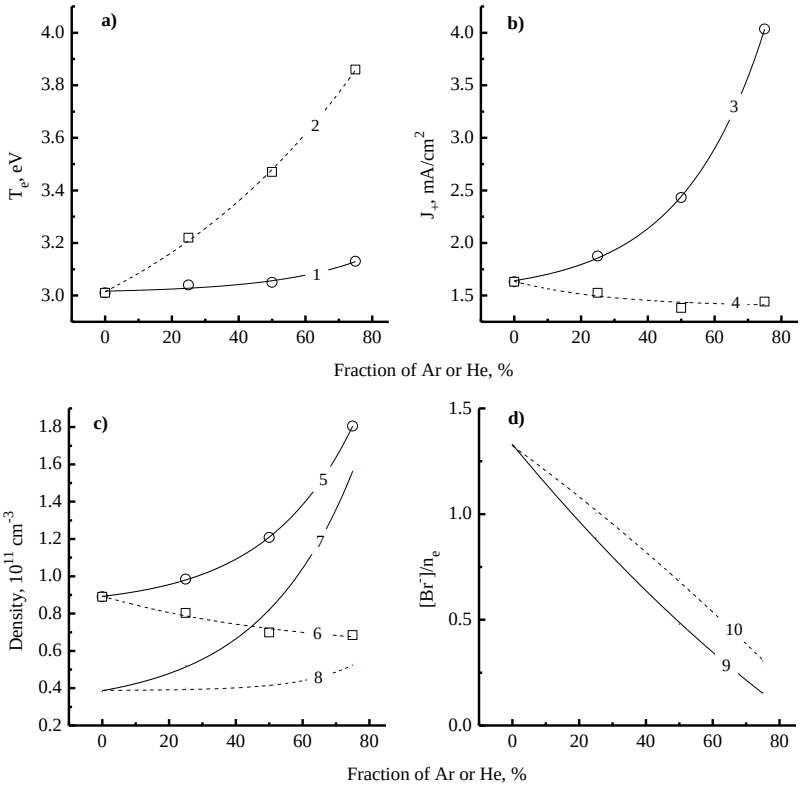

Fig. 1. Electrons- and ions-related plasma parameters in HBr + Ar (solid lines) and HBr + He (dashed lines) mixtures: 1, 2 – electron temperature; 3, 4 – ion current density; 5, 6 – total positive ion density; 7, 8 – electron density; 9, 10 – relative density of negative ions characterizing plasma electronegativity

Рис. 1. Параметры электронной и ионной компонент плазмы в смесях HBr + Ar (сплошные линии) и HBr + He (пунктирные линии): 1, 2 – температура электронов; 3, 4 – плотность ионного тока; 5, 6 – суммарная концентрация положительных ионов; 7, 8 – концентрация электронов; 9, 10 – относительная концентрация отрицательных ионов, характеризующая электроотрицательность плазмы

When analyzing kinetics of neutral species, we surely confirmed all principal features of HBr plasma

known from published works [14–16]. In particular, it was found that the total Br atom formation rate is almost equally contributed by R4: HBr + e → H + Br + e and R5: Br_2 + e → 2Br + e. The noticeable role of R5 is due to both $k_5 >> k_4$ (~ $1.1 \cdot 10^{-8}$ cm^3/s vs. ~ $1.6 \cdot 10^{-9}$ cm^3/s at T_e = 3 eV) and sufficient density of Br_2 molecules provided by R6: Br + Br → Br_2 on chamber walls. Accordingly, heterogeneous processes R6 and R7: Br + H → HBr represent dominant loss pathways for bromine atoms. On the contrary, the loss of atomic hydrogen mainly occurs in gas-phase reactions R8: H + HBr → H_2 + Br and R9: H + Br_2 → HBr + Br. As both reactions also produce Br atoms, the condition of [Br] >> [H] reasonably takes place (Fig. 2(a)). In addition, the effective replication of HBr molecules in R6 and R8 causes their domination over other neutral components.

The combination of HBr with Ar or He does not modify the chemistry of neutral species itself (as no new reactions appear in a kinetic scheme, except the ionization of Ar or He atoms), but influences kinetics of all electron-impart processes through changes in T_e and n_e. As a result, the intensification of dissociative collision of electrons with HBr ($k_4 n_e$ = 60–269 s^{-1} at 0–75% Ar and 60–140 s^{-1} at 0–75% He) and Br_2 ($k_5 n_e$ = = 408–1750 s^{-1} at 0–75% Ar and 408–1750 s^{-1} at 0–75% He) molecules with increasing fractions of both carrier gases takes place. In the case of HBr + He plasma, this effect is completely compensated by decreasing [HBr] and [Br_2] values, so that the Br atom density demonstrates the proportional decrease together with a growth of y_{He} (by ~ 3 times at 0–75% He, see Fig. 2(a)). At the same time, the stronger change of n_e in HBr + Ar plasma leads to the noticeable growth of dissociation degrees for HBr and Br_2 molecules. Accordingly, related effects are the deeper fall in their densities as well as the slower-than-linear (by ~ 2 times at 0–75% Ar, see Fig. 2(a)) decrease in Br atom density. Though similar mechanisms also influence H atoms kinetics, the actual [H] value mainly depends on the disturbance of loss processes, R7 and R8. That is why a decrease in corresponding loss rates together with [HBr] and [Br_2] produces either a constancy (in the case of HBr + He) or an increase (in the case of HBr + Ar) in H atom density. From Fig. 2(b), it can be seen also that a) the dominant positive ion up to 50% Ar or He is HBr^+, as it appears from the ionization of dominant neutral component; and b) the density of Ar^+ is much higher compared with He^+ at $y_{Ar} = y_{He}$. In fact, as the He fraction in a feed gas rises up to 75%, the [He^+] value even did not reach the level of bromine-containing counterparts. Such situation is due to the very low rate coefficient for R10: He + e → He^+ + 2e (~ $2.7 \cdot 10^{-12}$ cm^3/s at T_e = 3 eV) compared with R11: Ar + e → Ar^+ + 2e (~ $2.5 \cdot 10^{-10}$ cm^3/s at T_e = 3 eV). Another important feature is that effective ion masses in both gas systems are very close. Therefore, differences in ion bombardment intensities under one and same plasma excitation conditions are only in ion fluxes and energies.

From etching experiments, it was found that the mixing of HBr with Ar or He causes monotonic decreases in ZnO etching rates, R, but the effect appears to be stronger in HBr + He plasma (64.3–33.9 nm/min at 0–75% Ar vs. 64.3–19.0 nm/min at 0–75% He, see Fig. 3(a)). In fact, the maximum difference between two gas systems corresponds at ~ 50% of carrier gas, where the ~ 1.6 times slower etching in He-containing environment takes place. The back look on Figs. 2(b) and 3(a) allows one to conclude that the behavior of ZnO etching rate always correlates with changes in Br atom flux while demonstrates the disagreement with ion flux, at least for HBr + Ar plasma. Such situation formally corresponds to the domination of chemical etching pathway which appears in a form of ion-assisted chemical reaction. The ion-assisted nature for the interaction of Br atoms with ZnO surface is predetermined by the low volatility of reaction products, $ZnBr_2$ compounds. The latter follows from the fact that corresponding melting and boiling points (394 ºC and 697 °C, respectively [18]) are much higher than the sample temperature.

In order to obtain more detailed information concerning ZnO etching mechanisms, we conducted a series of plasma diagnostics and etching experiments in pure inert gas plasmas and then, evaluated ZnO sputter yields, Y_{sp}, as the etching rate to ion flux ratios. Corresponding Y_{sp} values were found to be ~ 0.02 atom/ion in Ar plasma and 0.01 atom/ion in He plasma. Accordingly, calculations of chemical etching rates in the same manner as it was done in Refs. [16, 30]: $R_{chem} = R - R_{phys}$, where $R_{phys} = Y_{sp}\Gamma_+$, yielded 58.5–23.8 nm/min at 0–75% Ar vs. 58.5–13.7 nm/min at 0–75% He. In fact, this means that a) the contribution of ion-assisted chemical reaction to the total ZnO etching rate starts from ~ 90% as well as does not fall down below 70% in Ar- and He-rich plasmas; and b) a decrease in ZnO etching rate with increasing fraction of carrier gas is completely related to the change in R_{chem}.

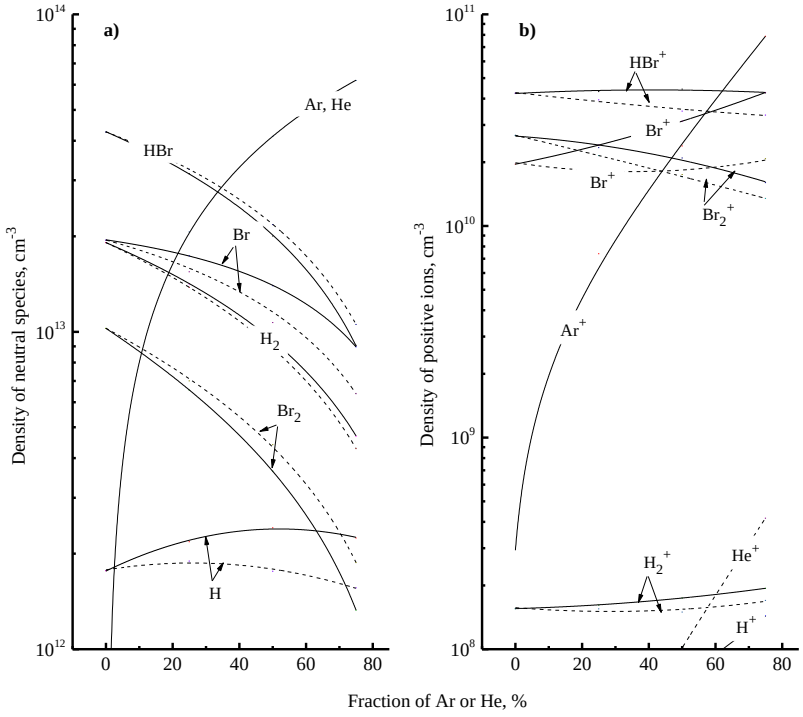

Fig. 2. Steady-state densities of neutral (a) and charged (b) species in HBr + Ar (solid lines) and HBr + He (dashed lines) plasmas
Рис. 2. Стационарные концентрации нейтральных (a) и заряженных (b) частиц в плазме HBr + Ar (сплошные линии) и HBr + He (пунктирные линии)

From Figs. 2(a) and 3(a), it can be understood also that a decrease in R_{chem} appears to be deeper compared with that for Br atom flux, $\Gamma_{Br} \approx$ $\approx 0.25[Br](k_B T_{gas}/\pi m_{Br})^{1/2}$. Such phenomenon surely reveal that the dilution of HBr by any carrier gas causes a decrease in effective reaction probability $\gamma_R = R_{chem}/\Gamma_{Br}$ (Fig. 3(b)). In our case, one can reasonably expect that the behavior of γ_R at constant surface temperature may be sensitive to the intensity of ion bombardment, as the latter provides the production of free adsorption sites for etchant species due to the ion-stimulated desorption of reaction products. From Figs. 3(c, d), it can be seen that increasing fraction of carrier gas lowers the negative ds bias voltage at W_{dc} = const, but causes opposite changes in the parameter $(m_i\varepsilon_i)^{1/2}\Gamma_+$, as follows from corresponding differences in ion fluxes, $\Gamma_+ \approx J_+/e$ (Fig. 1(b)). Therefore, HBr + Ar plasma exhibit the evident disagreement between γ_R and ion bombardment intensity, and the reason may be the presence of additional factor that inhibits the chemical activity of Br atoms. Obviously, the similar situation also takes place in HBr + He plasma, as there is no motivation to suggest different etching mechanisms in two chemically identical gas systems. In our opinion, a kind of "negative" effect may be caused by hydrogen atoms through their competitive adsorption on the ZnO surface. Obviously, these species cannot react with ZnO spontaneously because the Zn-O bond (~ 159 kJ/mol [18]) is much stronger compared with the Zn-H one (~ 85 kJ/mol [18]). That is why their chemical activity in respect to ZnO is much lower, and the increasing fraction of surface sites occupied by H atoms formally means the passivation of etched surface. From Fig. 2(a), it can be seen that HBr + He plasma is featured by [H] ≈ const and thus, exhibits no changes in surface passivation effect throughout 0–75% He. Accordingly, corresponding γ_R value simply follows the behavior of ion bombardment intensity, as follows from the change in $(m_i\varepsilon_i)^{1/2}\Gamma_+$. At the same time, both density and flux of of H atoms in HBr + Ar plasma demonstrate the growth toward higher y_{Ar} values (by ~ 1.4 times at 0–75% Ar, see Fig. 2(a)). As the latter directly means an increase in the fraction of "passivated" adsorption sites, a lack of adsorption sites for Br atoms may take place. Accordingly, this leads to a decrease γ_R in spite of increasing $(m_i\varepsilon_i)^{1/2}\Gamma_+$.

Of cause, we understand that above explanation has the somewhat speculative nature, as it was not confirmed directly by experiments. At the same time, our suggestions do not contradict with general regularities of plasma chemistry as well as provide the reasonable matching of ZnO etching kinetics with gas-phase plasma parameters. In fact, this demonstrates the advantage of model-based research schemes for obtaining more detailed information on etching mechanisms than it can be taken just from experiments.

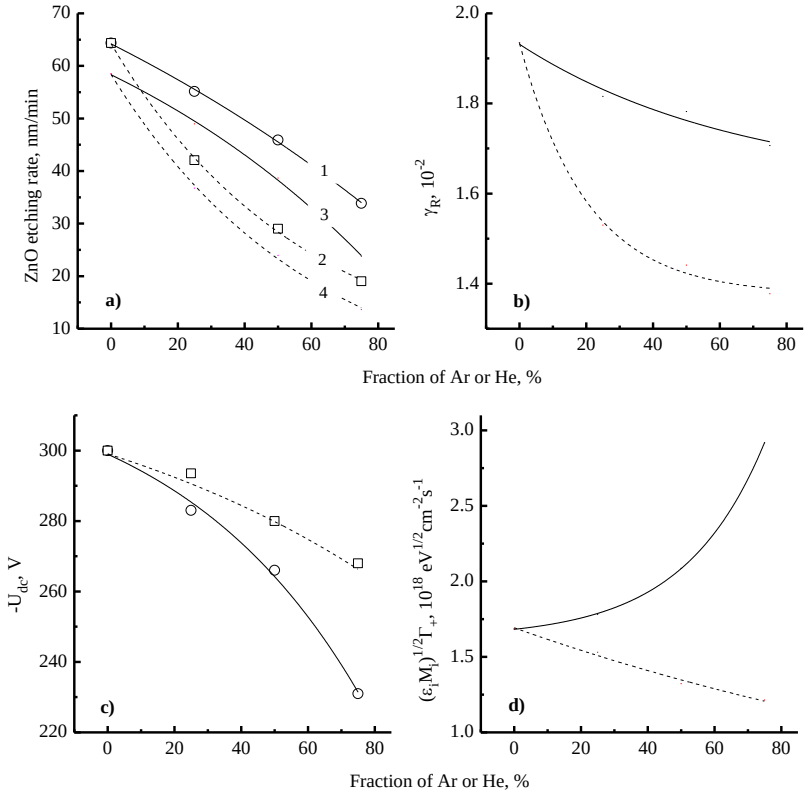

Fig. 3. ZnO etching kinetics and ion bombardment intensity in HBr + Ar (solid lines) and HBr + He (dashed lines) plasmas: a) ZnO etching rates (1, 2 – found in experiments; 3, 4 – ion-assisted chemical reaction); b) effective probability of ion-assisted chemical reaction; c) negative dc bias voltage; and d) parameter $(\varepsilon_i M_i)^{1/2}\Gamma_+$ characterizing the ion bombardment intensity.

Рис. 3. Кинетика травления ZnO и интенсивность ионной бомбардировки в плазме HBr + Ar (сплошные линии) и HBr + He (пунктирные линии): a) скорость травления (1 – полная, 2 – ионно-стимулированная химическая реакция); b) эффективная вероятность ионно-стимулированной химической реакции; c) отрицательное смещение на обрабатываемой поверхности; и d) параметр $(\varepsilon_i M_i)^{1/2}\Gamma_+$ характеризующий интенсивность ионной бомбардировки

CONCLUSIONS

The influence of inert carrier gases, Ar and He, on both gas-phase plasma characteristics and ZnO etching rate under conditions of reactive-ion etching process in the hydrogen bromide environment was analyzed. It was found that the dilution of HBr by any carrier gas always causes an increase in electron temperature (as increasing fraction of atomic species lowers the overall electron energy loss), reduces both absolute and relative density of negative ions (as decreasing fraction of electronegative component suppresses the rate of dissociative attachment) as well as leads to a growth of electron density. As the last effect appears to be much stronger for HBr + Ar plasma, corresponding consequence are the slower-than-linear fall of Br atom density (due to the intensification of electron-impact dissociation for both HBr and Br_2 molecules) as well as an increase in H atom density (due to decreasing their loss rates in $H + HBr \rightarrow H_2 + Br$ and $H + Br_2 \rightarrow$ $\rightarrow HBr + Br$ reaction pathways). At the same, the principal difference between Ar- and He-containing plasmas is the opposite effect of carrier gas on both ion flux and ion bombardment intensity. This phenomenon is due to opposite changes in total ionization rates determined by sufficient difference in ionization rate coefficients for Ar and He atoms. From the analysis of ZnO etching kinetics, it was concluded that the measured etching rate is mostly contributed by the ion-assisted chemical reaction. In both gas mixtures, the corresponding reaction rate decreases faster compare with the Br atom flux that corresponds to a decrease in the

effective reaction probability. In our opinion, the last phenomenon reflects changes in both ion bombardment intensity and hydrogen passivation effect.

The publication was made within the framework of the state task of the Federal State Institution Scientific Research Institute for System Analysis, Russian Academy of Sciences (conducting fundamental scientific research (47 GP)) on the topic No. 1023032900380-3-1.2.1 "Fundamental and applied research in the field of lithographic limits of semiconductor technologies and physicochemical processes of etching 3D nanometer dielectric structures for the development of critical technologies for the production of electronic components. Research and construction of models and designs of microelectronic elements in an extended temperature range (from -6 °C to +30 °C) (FNEF-2024-0004)".

The authors declare the absence a conflict of interest warranting disclosure in this article.

Публикация выполнена в рамках государственного задания Федерального государственного учреждения "Научно-исследовательский институт системного анализа Российской академии наук" (проведение фундаментальных научных исследований (47 НИР)) по теме № 1023032900380-3-1.2.1 "Фундаментальные и прикладные исследования в области литографского пределы возможностей полупроводниковых технологий и физико-химических процессов травления трехмерных нанометровых диэлектрических структур для разработки критических технологий производства электронных компонентов. Исследование и создание моделей и конструкций микроэлектронных элементов в расширенном диапазоне температур (от -6 °C до +30 °C) (FNEF-2024-0004)".

Авторы заявляют об отсутствии конфликта интересов, требующего раскрытия в данной статье.

REFERENCES
ЛИТЕРАТУРА

1. **Sugawara M.** Plasma etching. Fundamentals and applications. New York: Oxford University Press. 1998. 362 p.
2. Advanced plasma processing technology. New York: John Wiley & Sons Inc. 2008. 479 p.
3. **Wolf S., Tauber R.N.** Silicon Processing for the VLSI Era. V. 1. Process Technology. New York: Lattice Press. 2000. 416 p.
4. **Nojiri K.** Dry etching technology for semiconductors. Tokyo: Springer Internat. Publ. 2015. 116 p.
5. **Donnelly V.M., Kornblit A.** Plasma etching: Yesterday, today, and tomorrow. *J. Vac. Sci. Technol.* 2013. V. 31. P. 050825-48. DOI: 10.1116/1.4819316.
6. **Lieberman M.A., Lichtenberg A.J.** Principles of plasma discharges and materials processing. New York: John Wiley & Sons Inc. 2005. 757 p.
7. **Pearton S.J., Ren F., Fullowan T.R., Katz A., Hobson W.S., Chakrabarti U.K., Abernathy C.R.** Plasma etching of III–V semiconductor thin films. *Mater. Chem. Phys.* 1992. V. 32(3). P. 215-234. DOI: 10.1016/0254-0584(92)90203-k.
8. **Pearton S.J., Chakrabarti U.K., Lane E., Perley A.P., Abernathy C.R., Hobson W.S., Jones K.S.** Characteristics of III-V Dry Etching In HBr - Based Discharges. *J. Electrochem. Soc.* 1992. V. 139. P. 856-865. DOI: 10.1149/1.2069316.
9. **Bestwick T.D., Oehrlane G.S.** Reactive ion etching of silicon using bromine containing plasmas. *J. Vac. Sci. Technol. A.* 1990. V. 8. P. 1696-1701. DOI: 10.1116/1.576832.
10. **Jin W., Vitale S.A., Sawin H.H.** Plasma-surface kinetics and simulation of feature profile evolution in Cl_2+HBr etching of polysilicon. *J. Vac. Sci. Technol.* 2002. V. 20. P. 2106-2114. DOI: 10.1116/1.1517993.
11. **Pargon E., Menguelti K., Martin M., Bazin A., Chaix-Pluchery O., Sourd C., Derrough S, Lill T., Joubert O.** Mechanisms involved in HBr and Ar cure plasma treatments applied to 193 nm photoresists. *J. Appl. Phys.* 2009. V. 105. P. 094902. DOI: 10.1063/1.3116504.
12. **Kim D. K., Kim Y. K., Lee H.** A study of the role of HBr and oxygen on the etch selectivity and the post-etch profile in a polysilicon/oxide etch using HBr/O2 based high density plasma for advanced DRAMs. *Mater. Sci. Semicond. Proc.* 2007. V. 10(1). P. 41-48. DOI: 10.1016/j.mssp.2006.08.027.
13. **Cunge G., Kogelschatz M., Joubert O., Sadeghi N.** Plasma-wall interactions during silicon etching processes in high-density HBr/Cl_2/O_2 plasmas. *Plasma Sources Sci. Technol.* 2005. V. 14(2). P. S42-S52. DOI: 10.1088/0963-0252/14/2/S06.
14. **Efremov A., Kim Y., Lee H. W., Kwon K.-H.** A Comparative Study of HBr-Ar and HBr-Cl2 Plasma Chemistries for Dry Etch Applications. *Plasma Chem. Plasma Proc.* 2011. V. 31(2). P. 259-271. DOI: 10.1007/s11090-010-9279-7.
15. **Efremov A., Lee J., Kwon K.-H.** A comparative study of CF_4, Cl_2 and HBr+Ar inductively coupled plasmas for dry etching applications. *Thin Solid Films.* 2017. V. 629. P. 39-48. DOI: 10.1016/j.tsf.2017.03.035.
16. **Ефремов А.М., Бетелин В.Б., Kwon K.-H.** О сравнении механизмов реактивно-ионного травления SiO_2 и Si_3N_4 в плазме HBr + Ar. *Изв. вузов. Химия и хим. технология.* 2023. Т. 66. Вып. 6. С. 37-45. DOI: 10.6060/ivkkt.20236606.6786.
Efremov A.M., Betelin V.B., Kwon K.-H. On the comparison of reactive-ion etching mechanisms for SiO_2 and Si_3N_4 in HBr + Ar plasma. *ChemChemTech. [Izv. Vyssh. Uchebn. Zaved. Khim. Khim. Tekhnol.]*. 2023. V. 66. N 6. P. 37-45 DOI: 10.6060/ivkkt.20236606.6786.
17. **Efremov A.M., Smirnov S.A., Betelin V.B., Kwon K.-H.** Mechanisms of Plasma Etching of Titanium, Indium, Tin and Zinc Oxides in a Mixture of HBr + Ar. *Russ. Microelectronics*. 2021. V. 50. N 6. P. 379-386. DOI: 10.1134/S1063739721060068.
18. CRC Handbook of Chemistry and Physics. New York: CRC Press. 2010. 2760 p.
19. **Gul B., Rehman A.-ur.** A comparative study of capacitively coupled HBr/He, HBr/Ar plasmas for etching applications: Numerical investigation by fluid model. *Physics of Plasmas*. 2015. V. 22. P. 103520(1-9). DOI: 10.1063/1.4934922.

20. **Vyas S.** A Short review on properties and applications of ZnO based thin film and devices. *Johnson Matthey Technol. Rev.* 2020. V. 64(2). P. 202-218. DOI: 10.1595/205651320X15694993568524.
21. **Gartner M., Stroescu H., Mitrea D., Nicolescu M.** Various Applications of ZnO Thin Films Obtained by Chemical Routes in the Last Decade. *Molecules*. 2023. V. 28. P. 4674(1-27). DOI: 10.3390/molecules28124674.
22. **Shun'ko E.V.** Langmuir probe in theory and practice. Boca Raton: Universal Publ. 2008. 245 p.
23. **Cunge G., Ramos R., Vempaire D., Touzeau M., Neijbauer M., Sadeghi N.** Gas temperature measurement in CF_4, SF_6, O_2, Cl_2, and HBr inductively coupled plasmas. *J. Vac. Sci. Technol. A.* 2009. V. 27(3). P. 471-478. DOI: 10.1116/1.3106626.
24. **Celik Y., Aramaki M., Luggenholscher D., Czarnetzk U.** Determination of electron densities by diode-laser absorption spectroscopy in a pulsed ICP. *Plasma Sources Sci. Technol.* 2011. V. 20. P. 015022(1-12). DOI: 10.1088/0963-0252/20/1/015022.
25. **Efremov A.M., Kim G.H., Kim J.G., Bogomolov A.V., Kim C.I.** On the applicability of self-consistent global model for the characterization of Cl_2/Ar inductively coupled plasma. *Microelectron. Eng.* 2007. V. 84. P.136-143. DOI: 10.1016/j.mee.2006.09.020.
26. **Meeks E., Ho P., Ting A., Buss R.J.** Simulations of BCl_3/Cl_2/Ar plasmas with comparisons to diagnostic data. *J. Vac. Sci. Technol. A.* 1998. V. 16. P. 2227-2239. DOI: 10.1116/1.581332.
27. **Hsu C.C., Nierode M.A., Coburn J.W., Graves D.B.** Comparison of model and experiment for Ar, Ar/O_2 and Ar/O_2/Cl_2 inductively coupled plasmas. *J. Phys. D Appl. Phys.* 2006. V. 39. N 15. P. 3272-3284. DOI: 10.1088/0022-3727/39/15/009.
28. **Raju G.G.** Gaseous electronics. Tables, Atoms and Molecules. Boca Raton: CRC Press. 2012. 790 p.
29. **Christophorou L.G., Olthoff J.K.** Fundamental electron interactions with plasma processing gases. New York: Springer Science+Business Media LLC. 2004. 776 p.
30. **Ефремов А.М., Бетелин В.Б., Медников К.А., Kwon K.-H.** Параметры газовой фазы и режимы реактивно-ионного травления Si и SiO_2 в бинарных смесях Ar + CF_4/C_4F_8. *Изв. вузов. Химия и хим. технология*. 2021. Т. 64. Вып. 6. С. 25-34. DOI: 10.6060/ivkkt.20216406.6377.
Efremov A.M., Betelin V.B., Mednikov K.A., Kwon K.-H. Gas-phase parameters and reactive-ion etching regimes for Si and SiO_2 in binary Ar + CF_4/C_4F_8 mixtures. *ChemChemTech [Izv. Vyssh. Uchebn. Zaved. Khim. Khim. Tekhnol.]*. 2021. V. 64. N 6. P. 25-34. DOI: 10.6060/ivkkt.20216406.6377.

Поступила в редакцию 01.03.2024
Принята к опубликованию 08.07.2024

Received 01.03.2024
Accepted 08.07.2024